SAND2019-2248R

Sandia National Laboratories

Operated for the U.S. Department of Energy
by National Technology and Engineering Solutions
of Sandia, LLC.

Albuquerque, New Mexico 87185

date: February 25, 2019

to: Distribution

from: Craig M. Tenney (6631), Kevin N. Long (1554), and Jamie M. Kropka (1853)

subject: Predictions of Yield Strength Evolution Due to Physical Aging of 828 DGEBA/DEA using the Simplified Potential Energy Clock Model[1]

Summary

The capability of the Simplified Potential Energy Clock Model (SPEC) to represent the uniaxial compression yield strength evolution under isothermal aging conditions is evaluated for a widely used epoxy thermoset encapsulation material, 828 DGEBA/DEA. A baseline model calibration is used from [1] and [2]. We note that this calibration did not consider yield strength behavior close to the glass transition temperature (T_g), but in this work, the model is exercised in this temperature range to evaluate the ability to predict changes in material response with aging as equilibrium is approached. Some model alterations were needed to remove negative Prony weights in the thermal and bulk relaxation function (f_1), which is chiefly responsible for aging in this analysis, but otherwise, the model was not altered.

Model predictions of yield stress evolution are quantitatively different compared with experiments, but the rate of change of yield stress with respect to aging time is in reasonable agreement with respect to experiments for the first 1000 hours of aging. After this aging time, the measured yield stress stops evolving, but the model continues to evolve for several more decades in time. Parametric studies and model alterations are considered to investigate how yield strength evolution predictions are affected by modeling choices. It is clear that the baseline calibration must be re-examined in order to represent the aging data quantitatively.

[1]Sandia National Laboratories is a multi-mission laboratory managed and operated by National Technology and Engineering Solutions of Sandia, LLC., a wholly owned subsidiary of Honeywell International, Inc., for the U.S. Department of Energy?s National Nuclear Security Administration under contract DE-NA0003525.

1 Introduction

The Sandia-developed Potential Energy Clock Model (PEC) and its simplification, the Simplified Potential Energy Clock Model (SPEC), have been used successfully to predict a variety of thermoset and thermoplastic thermal-mechanical phenomena relevant to component manufacturing and environmental qualification simulation [1] and [2]. Phenomena considered during the model development included:

1. Isotropy (both rubbery and viscous)
2. Time-Temperature Superposition (TTS) and Thermorheological Simplicity (TRS) for all relaxation functions
3. Independent shear and bulk relaxation functions
4. Equivalence of the bulk and thermal relaxation functions (such that only the shear and bulk relaxation functions are defined in the model).
5. A time shift factor that was both thermal and deformation history dependent with the key feature being that thermal, shear, and bulk histories affect the shift factor independently, and each is subject to its own fading memory

With these phenomena, the SPEC model is able to fit through calibration:

1. A time or frequency-domain measurement of the shear modulus spanning fully the glass transition
2. Williams-Landel-Ferry (WLF) time-temperature superposition of all relaxation process above the glass transition
3. The thermal strain history of the material as the polymer is cooled or heated through the glass transition.
4. Volume strain history dependence of the glass transition.
5. Glassy compression and/or tension stress-strain curves through yield at different temperatures

A SPEC model calibration for 828 DGEBA/DEA was provided originally in [1] for the more sophisticated Potential Energy Clock model (PEC) but then simplified into the SPEC framework in [2]. Some predictive successes were demonstrated in those works and subsequent studies:

1. Thermal strain history under cyclic conditions across the glass transition [Kurtis Ford *unpublished*]

2. Creep under uniaxial tension conditions at temperatures below the glass transition
3. Tensile vs. compressive yield under uniaxial stress conditions
4. Volume change during uniaxial tension in the glassy state

Some efforts were made to predict the yield strength evolution under uniaxial compression of a DGEBA/poly(propylene oxide) epoxy glass [9] under different physical aging conditions (where the polymer was cooled into the glassy state and held for extended periods of time before testing). Model predictions appeared to be reasonable. However, a key feature of all calibration and prediction efforts of glass forming materials is that the thermal-mechanical history must be known and modeled precisely, and such information may not have been sufficiently known from the prior literature. Consequently, model efficacy is difficult to assess. Are differences from boundary conditions between experiments and simulations? Or are differences related a poor model calibration? Or do they arise from model form error, which is the inability of the constitutive model to represent certain kinds of thermal-mechanical behaviors?

To resolve these questions, we investigate how well the SPEC model can predict compressive yield stress evolution under prescribed thermal-mechanical aging conditions using a common Sandia encapsulation material, 828 DGEBA / DEA. A material specific calibration of the SPEC model exist for 828 DGEBA / DEA, and a suite of aging experiments showed significant changes in the material response with aging time [3]. Here, we compare model predictions to these data. The boundary conditions are well known experimentally and reproduced in the simulations as discussed in the next section. The only model calibration adjustment was to the volumetric relaxation function. Four Prony times (longer than any in the baseline spectrum) were added to remove negative Prony weights that were present in the baseline calibration. This adjustment ensures relaxation behavior consistent with the second law of thermodynamics. The implication of this change on the predictions herein will be discussed in a later section.

The memo is outlined as follows. In section 2, the experimental work is briefly summarized with the goal of describing information needed for the model comparisons. The main body of the memo is section 3. There, the simulation approach and baseline predictions (subsection 3.1) are presented and compared with experiments. Then, in subsection 3.2, sensitivities of specific model parameters associated with the non-linear material clock are investigated with respect to various aging metrics mainly to determine how sensitive model calibration choices are to predictions of aging behavior. A discussion of this body of results is then presented in 4, and an executive summary is provided at the opening of the memo.

2 Aging Experiments Recapitulation

The epoxy investigated was a diglycidyl ether of bisphenol-A (DGEBA), EPON 828, acquired from Miller-Stephenson and cured with diethanolamine (DEA) obtained from Fisher Scientific, hereafter referred to as DGEBA/DEA. The epoxy, EPON 828, has an epoxide

equivalent weight of 185-192 g/eq. DEA has a chemical formula of $HN(CH_2CH_2OH)_2$ and a molecular weight of 105.14 g/mole. The mix ratio of DGEBA:DEA was 1:0.12 parts by weight (pbw). Reagents are heated to 70C before mixing and held at 70C for about 5-10 min after mixing, while the initial adduct is formed by reaction of the secondary amine with epoxide. The adduct then slowly continues to react at 70C through various reaction paths over the course of 24 hours, at which point it will have reacted to a similar extent as in applications. In the present study, the epoxy in this state of cure is considered the unaged material. The cure parameters were chosen to obtain a similar extent of cure to production conditions. Additional processing and reaction details are provided elsewhere [6].

After the solution becomes transparent, the liquid is degassed down to 1.5torr for 3 minutes to remove bubbles. Care is taken to avoid volatizing uncoupled DEA molecules at low pressures and high temperatures. Cylinders are then poured using 10mL syringes (with the bottom orifice sealed) as molds with a diameter of 0.56in. Once the DGEBA/DEA had cured, the samples were removed from the molds and inspected for defects. Samples were then sectioned with a water-cooled diamond saw to a length of 1.12in to maintain as aspect ratio of 2:1. Each cylinder was individually inspected with parallel plates to ensure it was a right cylinder. Samples were then annealed at 105 C for 30 minutes and cooled at 0.8 C/min to room temperature. Samples were annealed 35 C above Tg to remove residual stresses and so every sample had the same initial thermal history. The cooling rate was chosen to decrease the temperature gradient across the sample while still being performed at a reasonable timescale. Freshly annealed and cooled samples are referred to as being in the "unaged" state. Although not truly "unaged", it is a small degree of aging compared to subsequent experiments, and it is kept consistent across all samples [5]. Isothermal thermal aging was applied to the compression cylinder samples. After the anneal and cooling processes, compression samples were placed into an oven at 55 C and aged for up to 10,000 hours (over 400 days). Once the set aging time for a specific sample set was reached, samples were either tested immediately, or stored in a freezer at -40 C until testing. Freezing and storing samples did not affect the measured stress-strain response.

After the compression samples were aged, individual cylinders were placed into a subpress in an environmentally controlled chamber on one of two thermally equilibrated Instron load frames (55R1125 or 5882, individually calibrated and verified) and allowed 30 minutes to equilibrate with the environmental chamber. The compression cylinders were tested at their respective aging temperatures. The subpress used in both instruments was a WTF-SP-34, which is compliant with ASTM D 695 Compressive Properties of Rigid Plastics. Samples were compressed at a crosshead speed of 0.1in/min, which translates to an initial strain rate of 0.893/min to a strain of approximately 15%. The yield stress was recorded as the local maxima immediately following the linear response of the material and preceding the flow or runaway region. Sample sets consisted of three to five samples and the variations in the yield stress across a single dataset were at most 2 MPa.

3 Simulations and Results

We used Sierra/Solid Mechanics Lagrangian Finite Element simulation package [10] with the *Universal_Polymer* (UPM) model [8] calibrated from references [2] and reproduced in the Appendix 1. We originally started with a model parameterization titled '828DEA_20160407Fit' but noted the presence of negative Prony weights in the thermal / volumetric relaxation function, f_1. This relaxation function is specified as a Williams-Watts stretched-exponential (WW) function as shown in Figure 1, and the constitutive model projects a Prony series onto that function. The negative Prony weights occur because, in the UPM model, only one set of Prony times are used for both relaxation function. Thus, when the shear Prony series is input directly, which typically occurs through the fitting of a shear master curve, the volumetric/thermal relaxation function uses the same Prony time basis even if this basis is not a good one for volumetric Prony series. This problem was fortuitously fixed by simply replacing several relaxation times not involved in the explicit specification of the shear relaxation spectrum (f_2) with values from an earlier model, '828DEA_MNFIT', that had no problems with negative Prony weights. Figure 1 shows the Prony series fit for f_1 to the WW function for the updated 828DEA model that removed negative Prony weights.

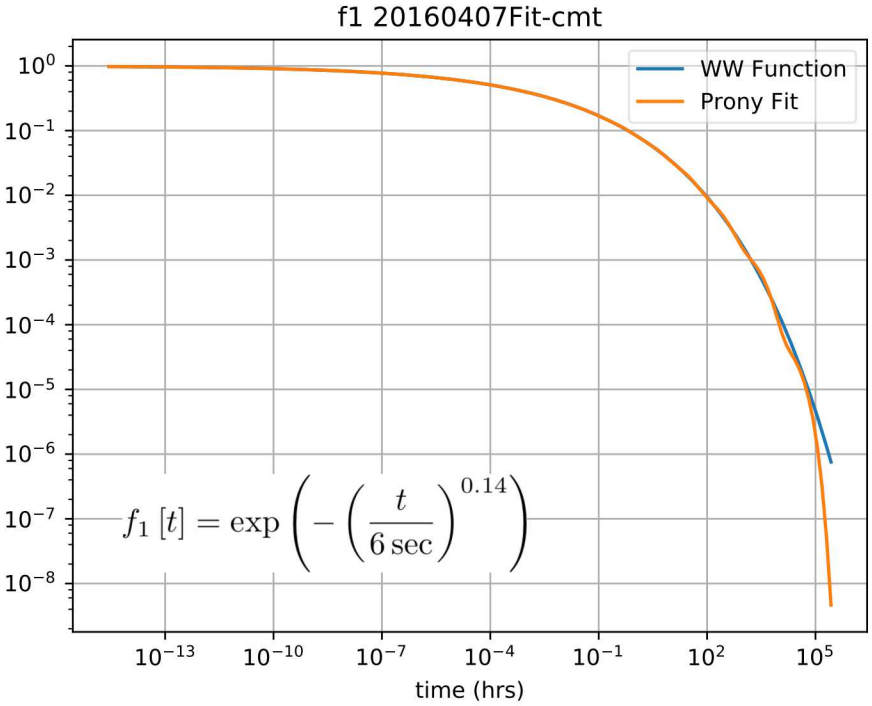

Figure 1. Prony series fit (with non-negative Prony weights) to the stretched exponential function that represents the 828/DEA volumetric relaxation function. The stretched exponential function is given with time units in seconds.

Simulations were constructed to mimic relevant experimental details as closely as possible. All simulations involved homogenous temperature and deformation fields such that a single eight-node hexahedral element with selective deviatoric integration scheme was used. Appro-

priate velocity and traction-free boundary conditions were applied to represent experimental conditions. All simulations in this study followed the same general test profile:

1. Anneal sample at 105 C.
2. Cool sample at 0.8 C/min to 25 C.
3. Rest sample at 25 C for one hour.
4. Age sample at 55 C for specified time (30 min heating time is included in total aging time).
5. Cool sample to 25 C over 30 minutes.
6. Rest sample at 25 C for one hour.
7. Heat sample to compression test temperature over 30 minutes.
8. Hold sample at test temperature and compress at a nominal rate of 0.089 min^{-1}.

Samples were unconfined except during the compression phase. Figure 2 shows a representative temperature profile for simulations of compression tests with aged samples. Simulations of unaged samples use the same general temperature profile, except with zero aging time and (possibly) a different test temperature.

Early simulation attempts used a combination of fixed time steps for most phases of the simulation, except aging, which used adaptive time stepping. This produced inconsistent results, due to integration problems at discontinuities in the temperature time rate of change profile. This difficulty was resolved by adding additional time blocks and using adaptive time stepping for all phases of the simulation, except the compression test. Because each new time block reverts to a specified initial time step, this strategy ensures sufficiently small time steps are used where the temperature profile changes abruptly.

The main input deck template is reproduced in Appendix 4 and the include file containing commands associated with creating output files in Appendix 1. Input decks for simulations of samples with, for example, different aging times were produced from the template via a bash script using sed to insert the required aging time value.

3.1 Baseline Physical Aging Predictions

Figure 3 shows nominal stress versus nominal strain for compression test experiments on samples with various aging times. For more consistent comparison, the initial non-linear beginning of each test was ignored, and all curves offset so that an extrapolation of the linear portion of the stress versus strain curve passes through the origin. This adjustment was made according to the location and value of the maximum of the tangent modulus of the stress versus strain curve.

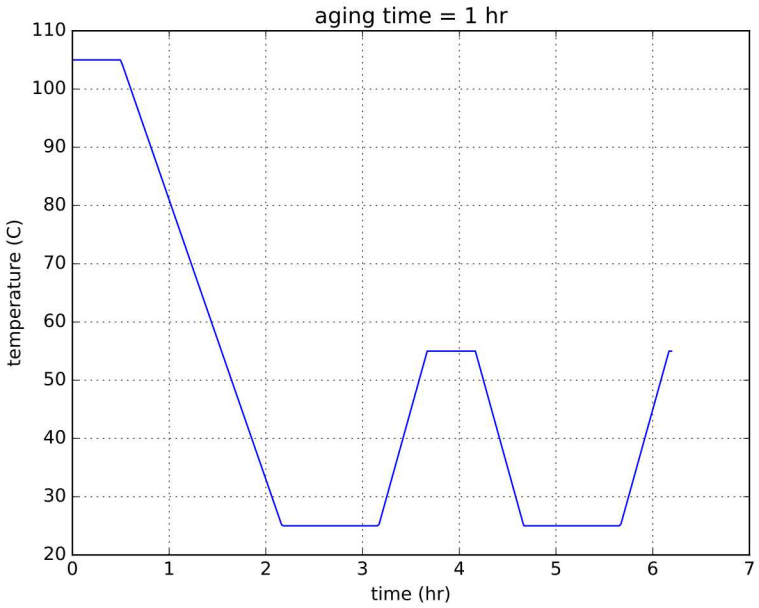

Figure 2. Representative temperature versus time profile for simulation with one-hour aged sample: anneal 0.5 hour at 105C, cool at 0.8C/min, rest one hour at 25C, age one hour at 55C (includes 30min heating time), cool for 30 min, rest one hour at 25C, heat for 30 min, and final compression test at 55C.

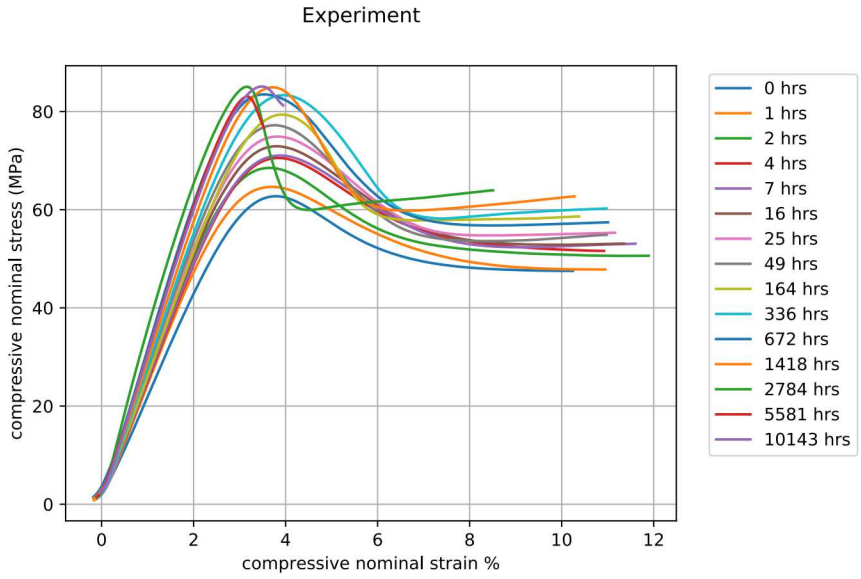

Figure 3. Experimental stress versus strain for compression tests on samples with various aging times.

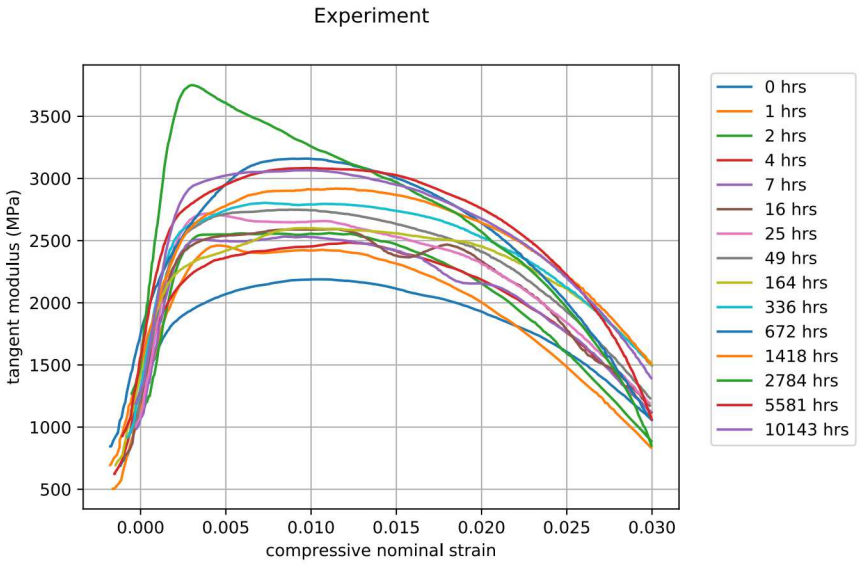

Figure 4. Experimental tangent modulus versus strain for compression tests on samples with various aging times.

Figure 4 shows tangent modulus versus nominal strain for compression test experiments on samples with various aging times. Calculation of the experimental tangent modulus versus strain was problematic since it involves taking finite difference derivatives on the somewhat noisy experimental data. Several strategies were tried with some success, before settling on a Gaussian-weight moving window average to smooth the experimental data. This smoothing method was checked to ensure it did not greatly alter the maximum stress value.

Figure 5 shows nominal stress versus nominal strain for compression test simulations on samples with various aging times. Consistent with experimental trends, simulation results show an expected increase in sample strength with increased aging time. Figure 6 shows tangent modulus versus nominal strain for compression test simulations on samples with various aging times. Tangent moduli at the start of compression are similar for all aging times. Close inspection shows that for the longest aging times, the maximum of the tangent modulus does not occur at the start of compression. This behavior was unexpected, and it could be related to the additional thermal history that occurs during cooling to 25 C, dwelling, and then reheating to the 55 C test temperature. No formal investigation has been attempted on this matter at this point.

Figure 7 compares yield stress versus aging time during compression between the experimental measurements and simulation predictions. Although offset from experimental results, simulation results show a similar linear dependence of yield stress versus the base ten logarithm of aging time, as measured by the slope of best-fit lines through all experimental data points.

If the best-fit line to experimental data considers only data points with aging times less than 1000 hours, it appears the experimental data reaches a plateau for longer times, which is

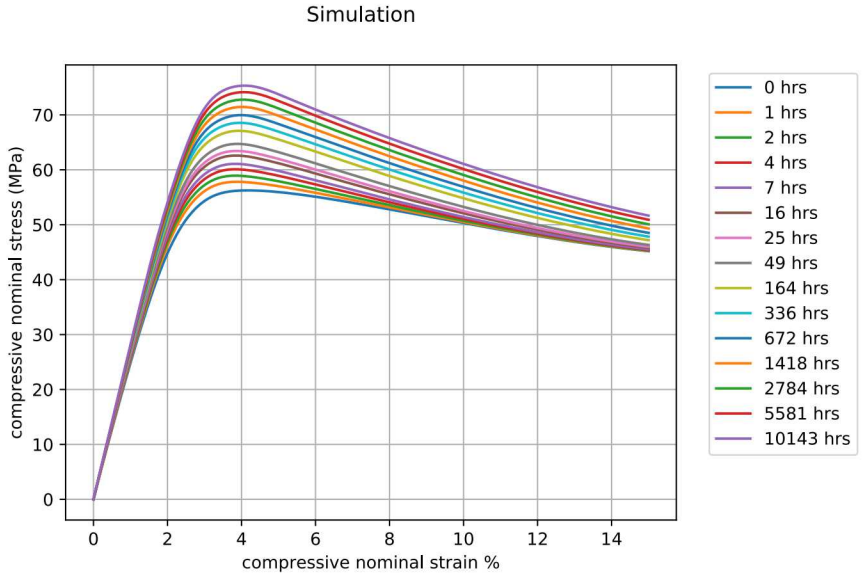

Figure 5. Simulated stress versus strain for compression tests on samples with various aging times.

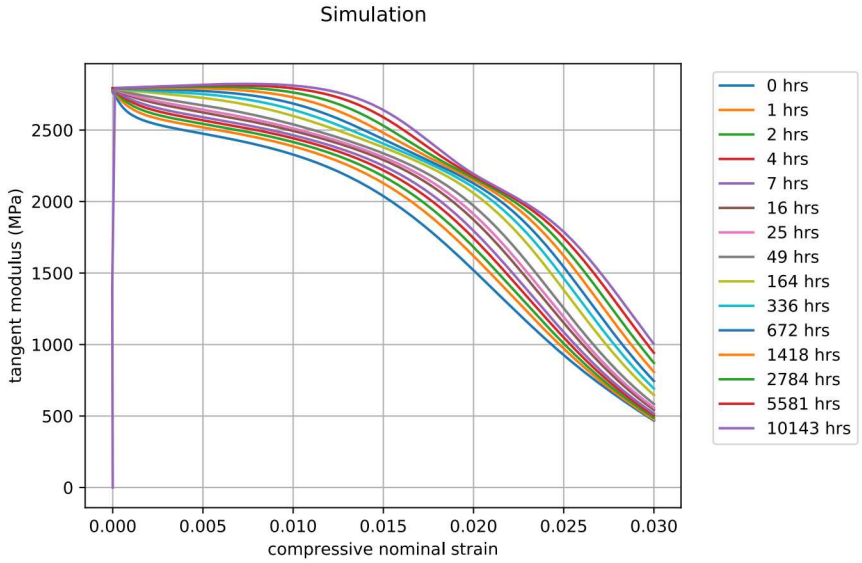

Figure 6. Simulated tangent modulus versus strain for compression tests on samples with various aging times.

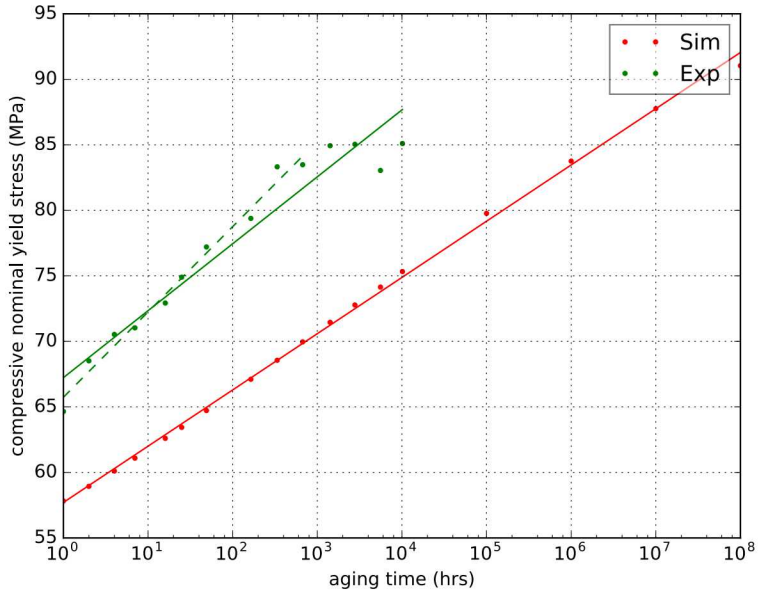

Figure 7. Comparison of yield stress versus aging time during compression between experimental measurements and simulation predictions. Lines are linear best fits to the data. Dashed line is best fit to experimental data for aging times less than 1000 hours.

expected physically. That is, given enough time, the glass can reach its equilibrated state with no subsequent time dependence. No plateau is seen for simulation results within the range of aging times considered.

Figure 8 compares yield strain versus aging time for compression test measurements and simulations. Yield strain is determined simply as the strain at which the maximum stress value occurs. For the experimental results, this yield strain value includes the strain offset described previously to eliminate the non-linear portion of the stress versus strain curves at the very beginning of each experimental run. While the simulation results show a minimum in the curve at aging times less than ten hours, the noisy experimental results suggest a possible decrease at the longest aging times. The cause of the apparent outlier simulation data point for an aging time of 1e6 hours is currently unknown but could be related to the density of simulation output and the post processing method.

Figure 9 shows $\log_{10}(a)$ versus aging time for the compression test simulations on samples with various aging times. The $\log_{10}(a)$ value shown is that at the start of the compression phase of the simulation, after the sample has been heated to the 55 C test temperature. $\log_{10}(a)$ values show a smooth and nearly linear increase with the base ten logarithm of aging time through the first 10,000 hours of aging. Using the time-weighted average shift factor (of approximately 100,000) over this time interval, this aging window exhausts the original volumetric relaxation function (from the '828DEA 20160407Fit'). That is, if you multiply this shift factor against any of the Prony times, that relaxation time scale is still

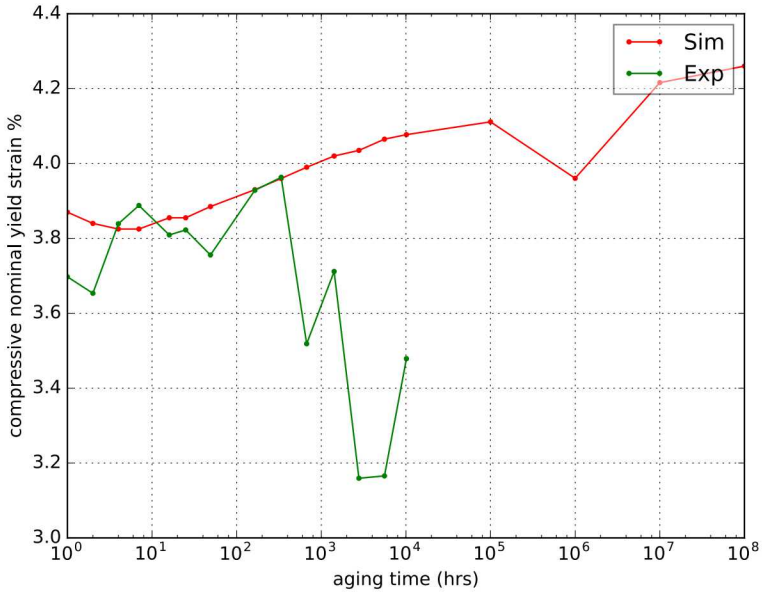

Figure 8. Comparison of yield strain versus aging time for compression test measurements and simulations.

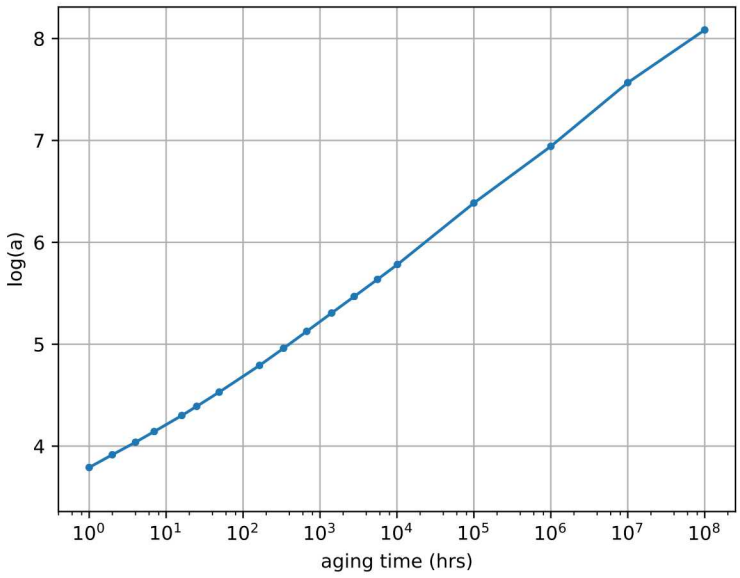

Figure 9. Simulated $\log_{10}(a)$ versus aging time for compression tests on samples with various aging times.

shorter than the aging time scale of 10,000 hours. However, as previously discussed, four longer time scale Prony times were added, which caused the Prony series projection onto the stretched exponential relaxation function not to have negative Prony weights. Although these extra times only account for about 2% of the relaxation function by magnitude, they are actively relaxing between 1E4 and 1E8 hours of aging.

Suppose that all the hereditary integrals in the shift factor equation relaxed and vanished. Under such conditions, the model would return to Williams-Landel-Ferry (WLF) behavior. For the material input deck in Appendix 1, at 55 C of aging, the base ten logarithm of the shift factor should equilibrate to near 9. The shift factor during aging is approaching this limit in Figure 9 at one hundred million hours of aging. After this time, the shift factor should remain constant. Since the shift factor would no longer change with aging time, the amount of shear deformation needed to accelerate the shift factor and realize yield would no longer change. This scenario appears to be reached experimentally in Figure 7 at a time scale of 1000 hours.

3.2 Non-Linear Parameter Sensitivity Studies on Aging Predictions

Using the model parameterization described previously and reproduced in Appendix 1 as a baseline, we investigated the sensitivity of simulation results to changes in two material clock parameters, C3 and C4. Simulation runs with C3 and C4 independently set to 90% and 110% of their baseline values (denoted 090C3, 090C4, 110C3, or 110C4, as appropriate) are compared below with the baseline results described in Section 3.1.

Figure 10 shows maximum tangent modulus versus aging time results from experiment and from simulations run using material models with various C3 and C4 parameter values. Neither C3 nor C4 alter the maximum tangent moduli calculated from simulations. This observation is expected. The simulation maximum tangent modulus occurs immediately when the compressive load begins when the shift factor is highest because the maximum number of Prony terms are incapable of relaxing. Here, nearly the fully glassy modulus is realized at the 55 C temperature. The slight difference in moduli with aging time manifests from just a few of the shortest Prony times changing from being able to relax (unaged–lower shift factor) to being unable to relax (aged–higher shift factor). The C4 parameter has no impact on the shift factor during the cool down aging steps in the simulations. The C3 parameter has a small influence on the shift factor behavior during cool down and aging, but apparently not enough to change the initial loading response. Simulations yield maximum tangent modulus values similar to those calculated from experiment, but as described previously, due to the noisy nature of the underlying experimental data, calculation of experimental tangent moduli was problematic, and there is much uncertainty with the experimental trend of increasing maximum tangent modulus versus aging time.

Figure 11 shows yield stress versus aging time results from experiment and from simulations run using material models with various C3 and C4 parameter values. Increasing C3 and decreasing C4 lead to noticeably increased yield stress values, with C4 being significantly more sensitive. The slope of the yield stress versus aging time lines remains generally unaltered

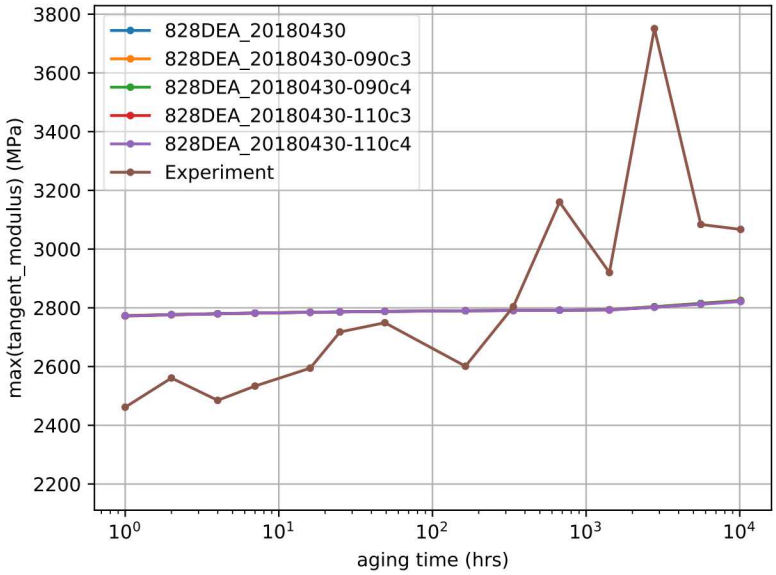

Figure 10. Maximum tangent modulus versus aging time results from experiment and from simulations run using material models with various C3 and C4 parameter values.

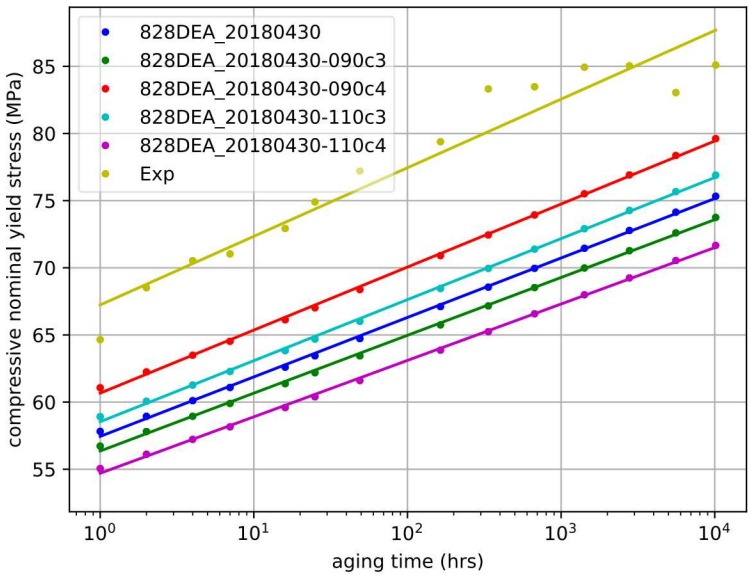

Figure 11. Yield stress versus aging time results from experiment and from simulations run using material models with various C3 and C4 parameter values.

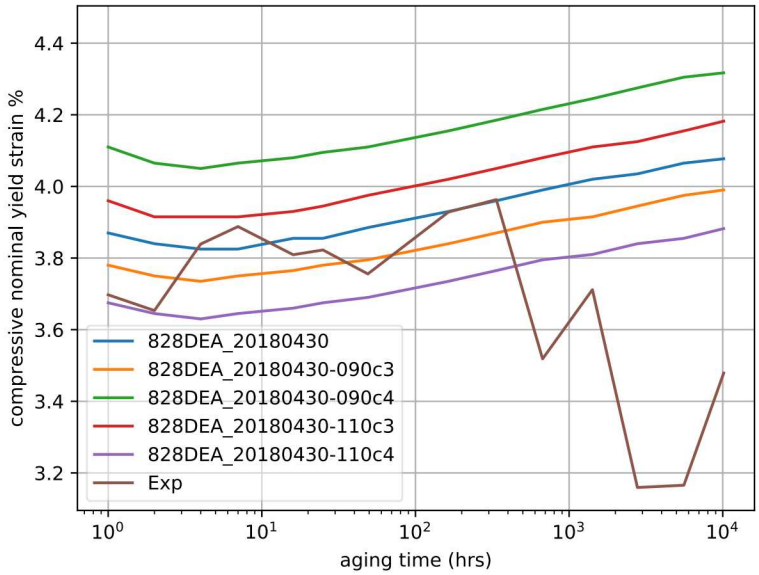

Figure 12. Yield strain versus aging time results from experiment and from simulations run using material models with various C3 and C4 parameter values.

with the changes in C3 and C4. Larger changes in C3 and/or C4 than those investigated would be necessary to match experimental results. While C3 could be changed to match these results at 55 C, historically, C4 has been used to tune the model prediction of yield. Considering the higher sensitivity of yield to C4, this appears to be the best approach. With such an approach, other material response predictions (e.g., temperature dependence of yield stress) must be checked when these parameter changes are made.

Figure 12 shows yield strain versus aging time results from experiment and from simulations run using material models with various C3 and C4 parameter values. Increasing C3 and decreasing C4 lead to noticeably increased yield strain values, with C4 being significantly more sensitive. While the yield strain versus aging time curves are offset for different values of C3 and C4, the overall curve shapes and local slopes remain generally unaltered. As described previously, calculation of experimental tangent moduli and yield strain values is made problematic by the inherently noisy underlying data.

Figure 13 shows $\log_{10}(a)$ versus aging time results from simulations run using material models with various C3 and C4 parameter values. These $\log_{10}(a)$ values are those at the start of the compression test. Changes in C3 resulted in very small changes to $\log_{10}(a)$ values at the shortest aging times. At the longest aging times, changes in C3 had negligible effect on $\log_{10}(a)$. Changes in C4 had no discernible effect on $\log_{10}(a)$ as expected.

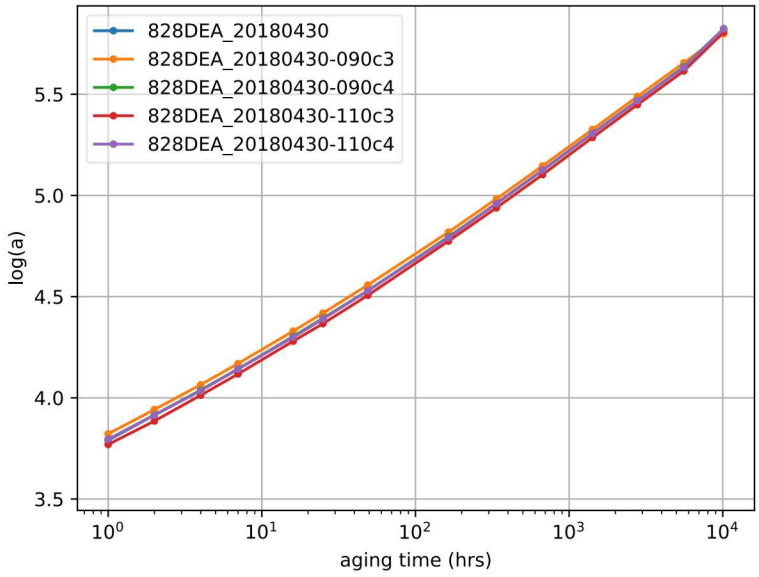

Figure 13. $\log_{10}(a)$ versus aging time results from simulations run using material models with various C3 and C4 parameter values.

3.3 Un-Aged Isothermal Compression Sensitivities to Changes in NLVE Parameters

Using the general simulation scheme described previously, simulations were run for unaged samples at five different compression test temperatures: -55C, 0C, 23C, 37C, and 59C. To test the sensitivity of results to changes in the C3 and C4 material clock parameters, simulations were repeated with C3 and C4 set to both their baseline values and 90% and 110% of baseline (denoted 090C3, 090C4, 110C3, or 110C4, as appropriate). Results at the various test temperatures for different C3 and C4 values are compared below.

Figure 14 shows stress versus strain results from simulations run at multiple temperatures using material models with various C3 and C4 parameter values. Experimental results can be found in [3].

Figure 15 shows maximum tangent modulus versus test temperature results from simulations run using material models with various C3 and C4 parameter values. Tangent moduli show the expected decrease with increasing temperature. Changes in C3 and C4 only slightly affect the results and only at the lowest temperatures.

Figure 16 shows yield stress versus test temperature results from experiment and from simulations run using material models with various C3 and C4 parameter values. Yield stress shows the expected decrease with increasing temperature. Increasing C3 and decreasing C4 lead to noticeably increased yield stress values, with C4 being significantly more sensitive. Yield stress values from simulation show a much greater temperature dependence than those

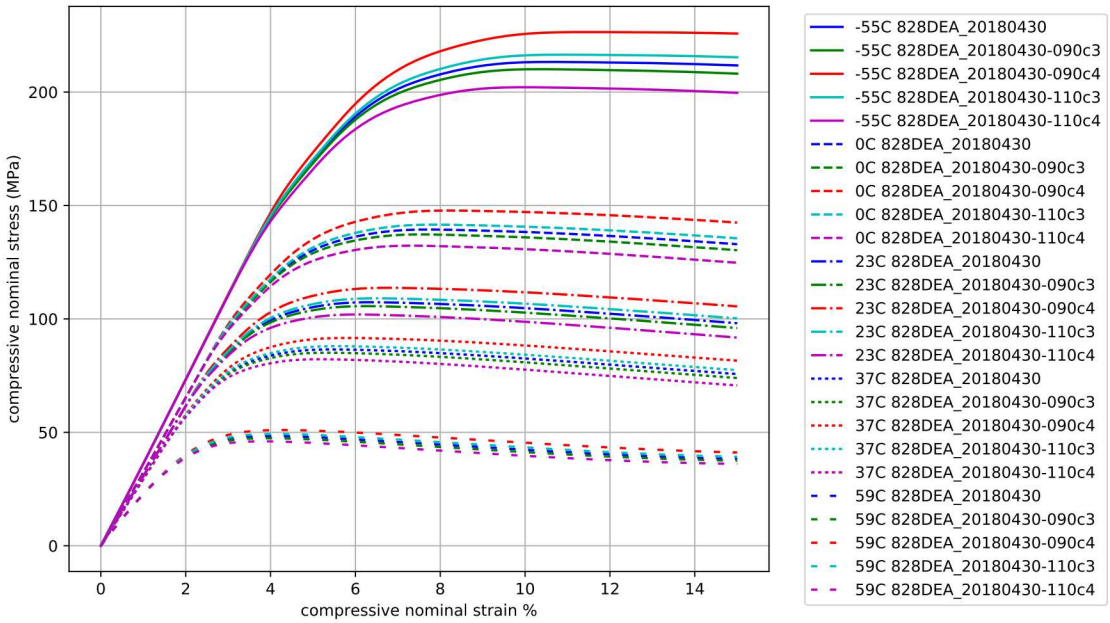

Figure 14. Unaged sample stress versus strain results from simulations run at multiple temperatures using material models with various C3 and C4 parameter values.

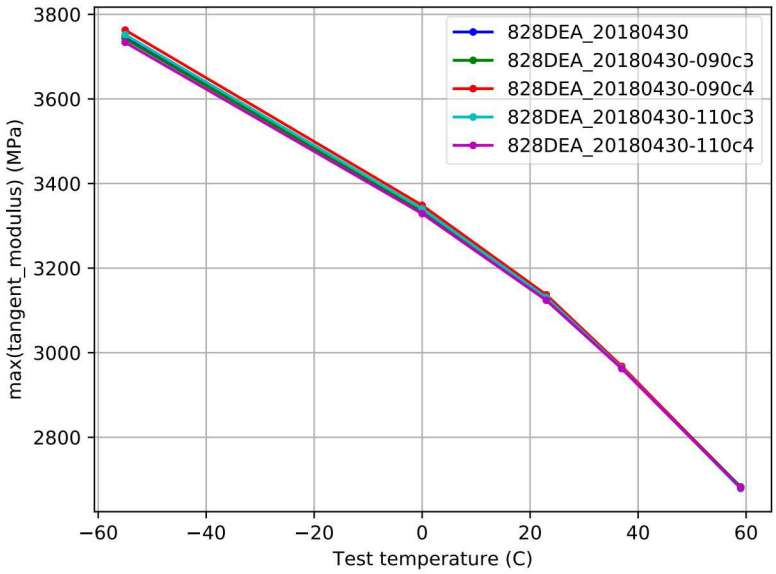

Figure 15. Unaged sample maximum tangent modulus versus test temperature results from simulations run using material models with various C3 and C4 parameter values.

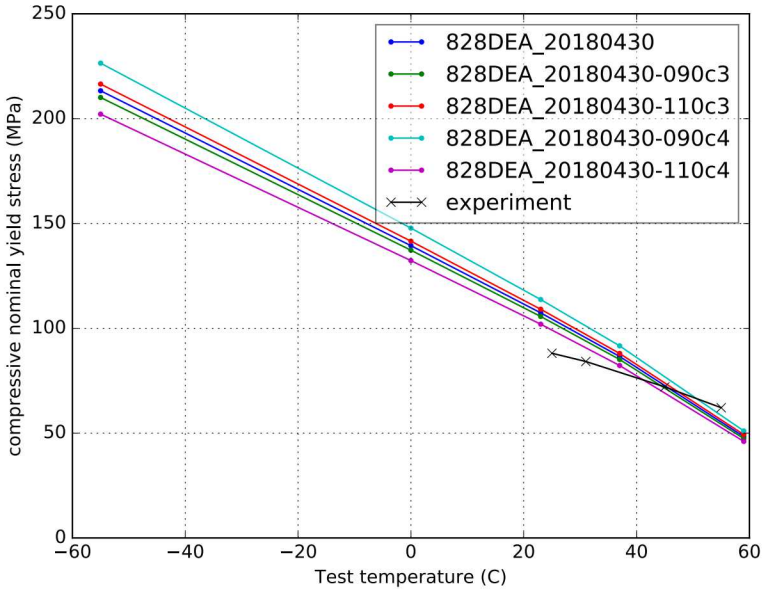

Figure 16. Unaged sample yield stress versus test temperature results from experiment and from simulations run using material models with various C3 and C4 parameter values.

measured during experiments. Best agreement between simulation and experiment occurs at approximately 45 C. Improvement could be made by changing the C4 parameter, which is usually set to match these data. However, the volumetric relaxation function and C3 play a role as they control the shift factor as the material is cooled deeper into the glass.

Figure 17 shows yield strain versus test temperature results from simulations run using material models with various C3 and C4 parameter values. Yield strain decreases with increasing temperature, predicting that the decrease in yield stress is dominant over the decrease in modulus in terms of where non-linear softening begins. Increasing C3 and decreasing C4 lead to noticeably increased yield strain values, with C4 being significantly more sensitive. This effect is most significant at the lowest temperatures, changing the slope of the yield strain versus temperature curve slightly with increasing temperature.

Figure 18 shows $\log_{10}(a)$ versus test temperature results from simulations run using material models with various C3 and C4 parameter values. As expected from the terms in the shift factor determination, C4 has no effect on the shift factor during aging as there is no shear deformation. C3 does influence the behavior of the shift factor during un-aged cooling although not so significantly in this range of C3 variation.

3.4 Truncation of F1 Prony series

A major model deficiency identified in comparing the yield strength evolution vs. isothermal aging time in Figure 7 is that the baseline calibration continues to evolve for many orders

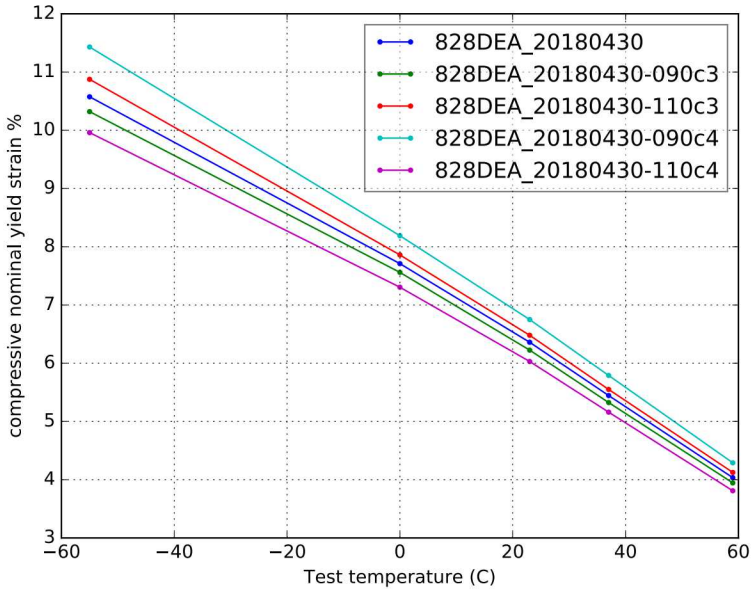

Figure 17. Unaged sample yield strain versus test temperature results from simulations run using material models with various C3 and C4 parameter values.

of magnitude in time beyond the experimental behavior. Indeed, as previously discussed, the model could only stop evolving if the equilibrated, C3-adjusted WLF time shift factor is reached, a $\log_{10} a \approx 9$.

In this section, we investigate a simple adjustment to the model. We truncate the volumetric relaxation function to force the model to equilibrate around the time the experiments equilibrate in the context of yield strength evolution. This can be accomplished by examining the baseline shift factor evolution in Figure 9. Equilibration occurs, by extrapolation, near 10^9 hours of aging in the model in that figure. Since, from Figure 7, we want the model to equilibrate after approximately 10^3 hours, we need to truncate the relaxation function by removing all times slower than $a_{\max} * \tau_{\max} > 1000$ hours. Here, $a_{\max} \approx 10^9$ such that $\tau_{\max}$ must be less than approximately 1 millionth of an hour. Figure 19 shows the f_1 Prony series curves for both the baseline 828DEA model and the modified model that eliminated (truncated) all Prony terms with relaxation times longer than 1.5e-3 seconds, chosen based on considerations above and the actual WLF equilibrated shift factor at 55 C. The truncated Prony series weights are normalized such that they add to one as required by the model.

Figure 20 shows $\log_{10}(a)$ versus aging time results from simulations run using baseline and truncated Prony series material models. The aging time at which $\log_{10}(a)$ for the truncated Prony series model reaches its limiting equilibrium value is consistent with the longest Prony series relaxation time retained in the truncated model and reasonably approximates the equilibration time seen experimentally from the standpoint of yield strength evolution with aging time. The limiting value for $\log_{10}(a)$ of approximately 10 for the truncated Prony

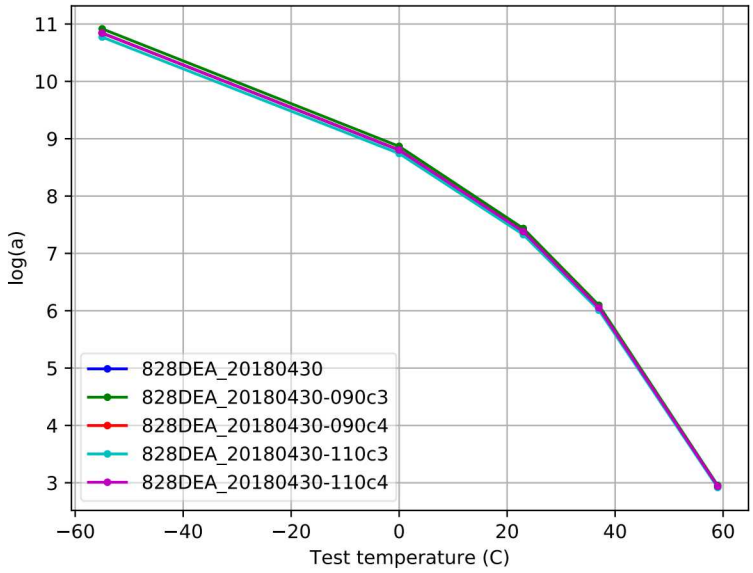

Figure 18. Unaged sample $\log_{10}(a)$ versus test temperature results from simulations run using material models with various C3 and C4 parameter values.

series model slightly exceeds the expected value of 9.6. The reason for this is unknown at this time.

Figure 21 shows yield stress versus aging time for experimental and for truncated Prony series material model compression tests on samples with various aging times. Unlike results from the baseline material model shown in Figure 7, the yield stress predicted by the truncated Prony series model starts at a much larger value and then does not significantly change (increase) with increased aging time.

Figure 22 shows $\log_{10}(a)$ at start of compression versus temperature for compression test simulations run using baseline and truncated Prony series material models. Figure 23 shows yield stress versus temperature from compression test simulations run using baseline and truncated Prony series material models. As with the aging time results described above, the truncated Prony series model results in significantly increased $\log_{10}(a)$ and yield stress values, relative to the baseline model.

An additional simulation was run for both the baseline and truncated Prony series models to investigate the thermal expansion behavior. These simulations began with a 30-minute annealing period at 140 C, immediately followed by cooling at 2 C/min to 0 C, immediately followed by reheating at 2 C/min back to 140 C. The temperature range and cooling and heating rates were chosen to match experiments discussed in [1]. Figure 24 shows thermal strain versus temperature during cooling and reheating at 2 C/min for simulations run using the baseline and truncated Prony series material models. As seen in the figure, the transition between rubbery and glassy states occurs at a lower temperature for the truncated Prony

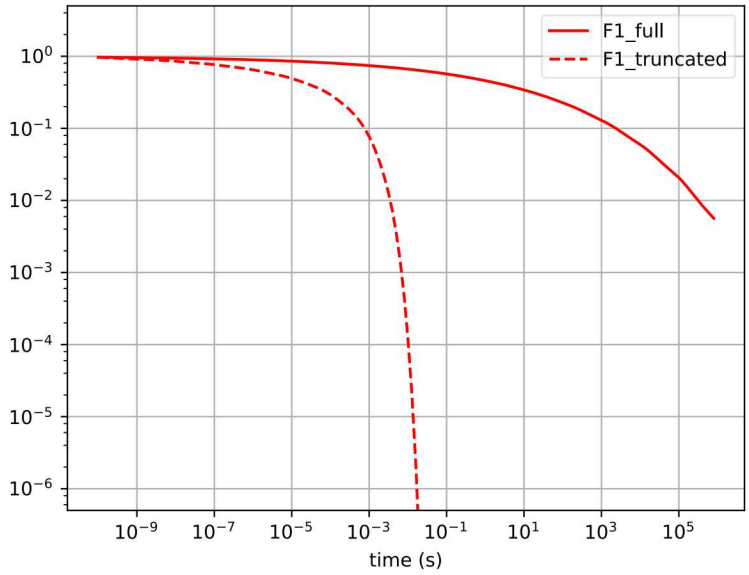

Figure 19. f_1 Prony series curves for both the baseline 828DEA model and the modified model that eliminated (truncated) all Prony terms with relaxation times longer than 1.5e-3 seconds.

series model. Figure 25 shows the coefficient of thermal expansion versus temperature during cooling and reheating at 2 C/min from experiment and for simulations run using the baseline and truncated Prony series material models.

Models and experiment all show hysteresis and a distinct overshoot of the initial cooling curve by the heating curve near the glass transition. The experimental results are bracketed by the two simulation models, neither of which can be said to be a distinctly better fit. This suggests an optimally fitted model would have a longest Prony series relaxation time somewhere between the baseline model and the truncated Prony series model used here. We note that some oscillations are observed during heating of both curves. The source of these oscillations has not been carefully investigated, but the oscillations do not change the contrast between the truncated vs. baseline model performance compared with the experiments.

4 Discussion

This work examines the performance of the baseline 828 DGEBA / DEA epoxy thermoset material model to predict compressive yield strength over a broad range of isothermal (55 C) sub-Tg aging times. The underlying physical mechanism for this change in behavior is physical aging, associated with densification and the continued loss of mobility in the molecular network. In the SPEC constitutive model, this loss of mobility is associated with the increase in the viscoelastic shift factor with aging time as shown in Figure 9. The baseline 828 DGEBA / DEA epoxy thermoset calibration predicts the change in yield strength over

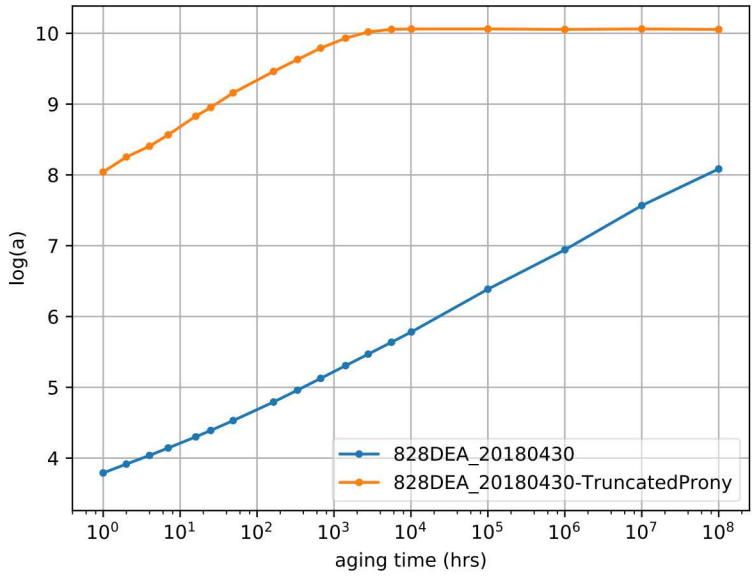

Figure 20. $\log_{10}(a)$ versus aging time results from simulations run using baseline and truncated Prony series material models.

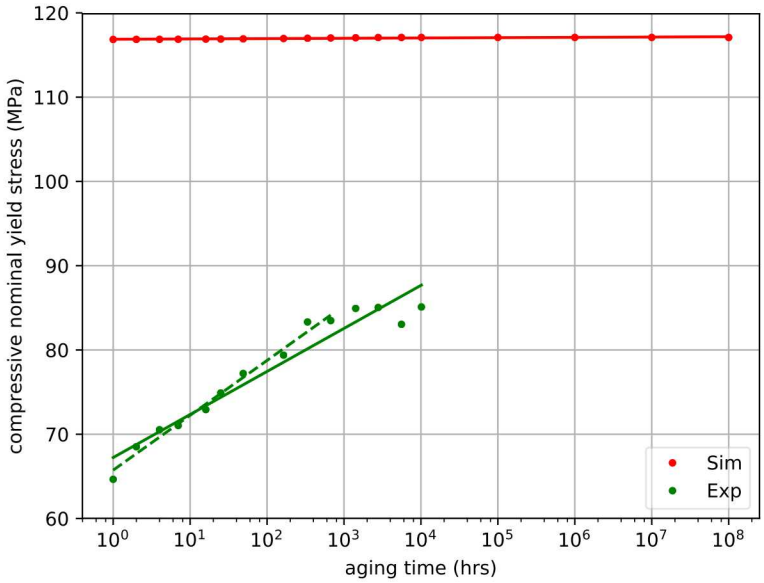

Figure 21. Yield stress versus aging time for experimental and for truncated Prony series material model compression tests on samples with various aging times. Lines are linear best fits to the data. Dashed line is best fit to experimental data for aging times less than 1000 hours.

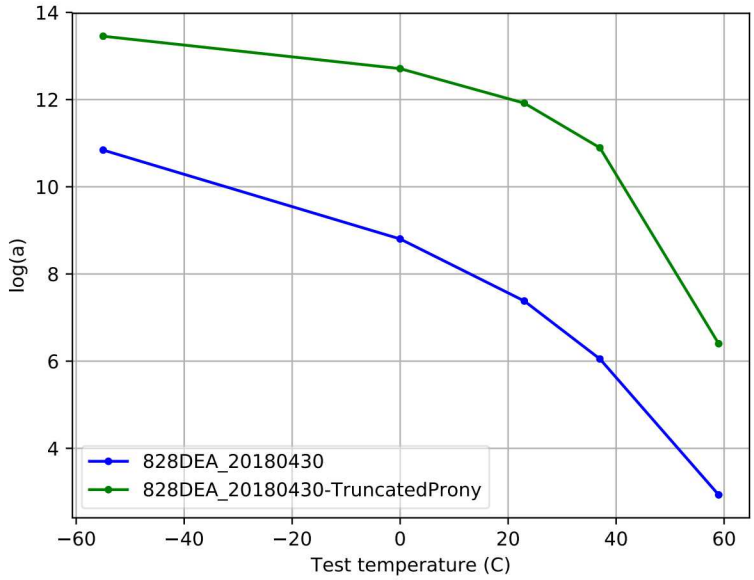

Figure 22. $\log_{10}(a)$ at start of compression versus temperature for compression test simulations run using baseline and truncated Prony series material models.

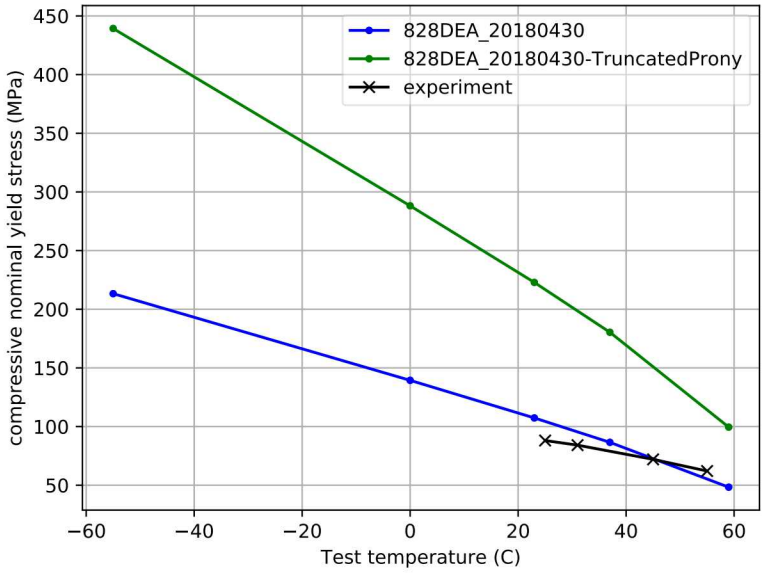

Figure 23. Yield stress versus temperature from compression test simulations run using baseline and truncated Prony series material models.

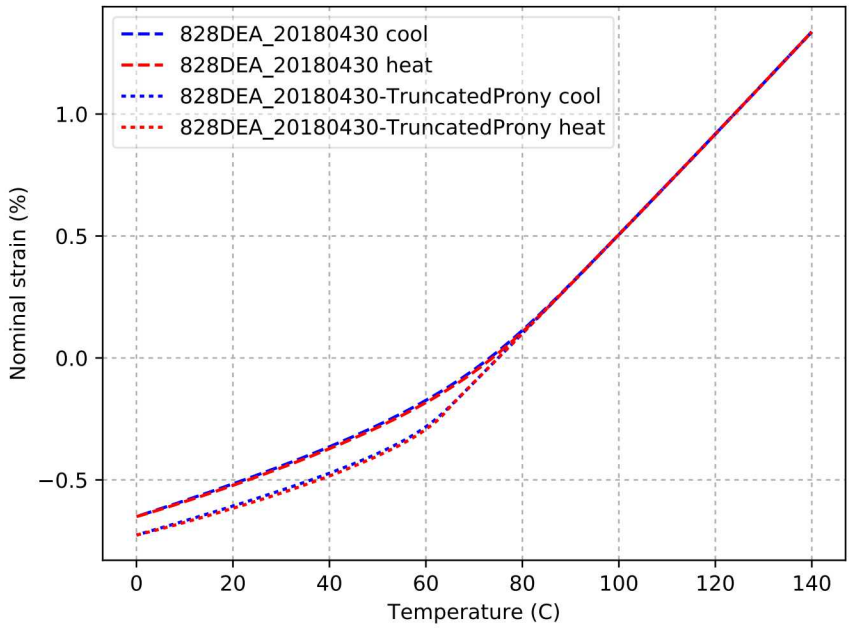

Figure 24. Thermal strain versus temperature during cooling and reheating at 2 C/min for simulations run using the baseline and truncated Prony series material models.

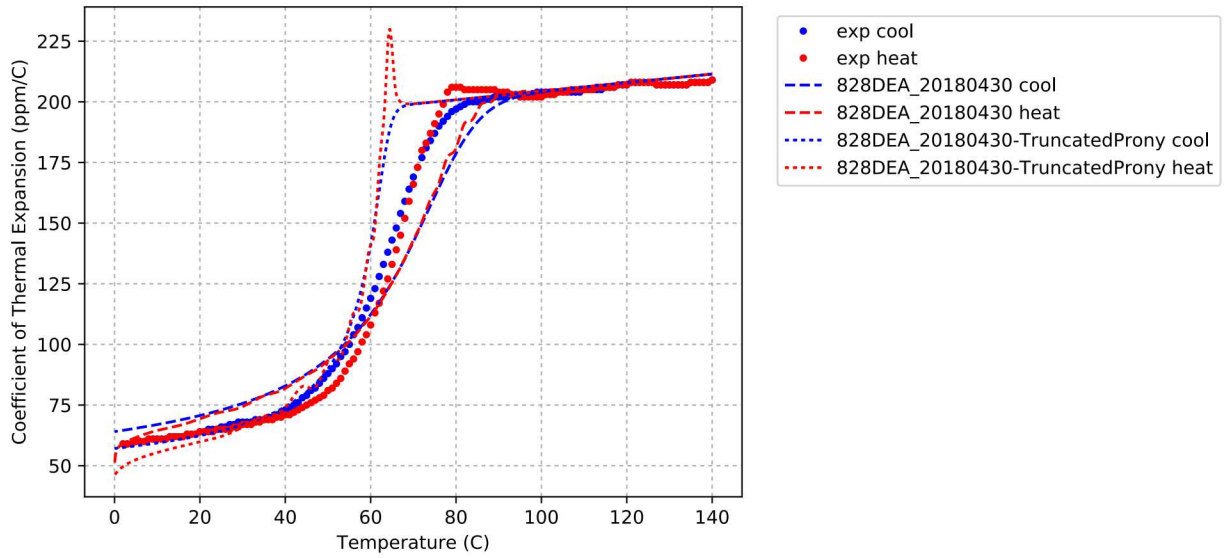

Figure 25. Coefficient of thermal expansion versus temperature during cooling and reheating at 2 C/min from experiment and for simulations run using the baseline and truncated Prony series material models.

time under isothermal physical aging conditions as shown by similar slopes in the first 1000 hours of 55 C isothermal aging in Figure 7.

Quantitatively, there are several shortcomings of the baseline model calibration, which is given in Appendix 1. First, un-aged yield strengths vs. temperature shown in Figure 16 demonstrate that the model calibration is different from experiments. Specifically, the slope of un-aged yield strength is steeper for the simulation than the experiments. This difference is related to the model calibration and suggests that a different combination of the volumetric/thermal relaxation function, parameter C3, and parameter C4 may be needed.

The next major issue is that the model does not predict the correct aging time associated with material equilibration after which no more changes to the yield strength are seen vs. aging time. Experimentally, this time is around 1000 hours. However, the simulations only start to equilibrate after 100,000,000 hours. That very significant difference appears to arise from the longest Prony times in the volumetric/thermal relaxation function (F_1 in the appendix), especially those longer than 100,000 seconds. Interestingly, these longer Prony times were not in the original baseline calibration and were added here in this work to eliminate non-thermodynamically admissible negative Prony weights that appeared during the projection of a Prony series onto the stretched exponential analytic function: $\mathrm{F}_1[x] = \exp\left(-\left(\frac{x}{\tau_1}\right)^{\beta_1}\right) \rightarrow \sum_i w_i \exp\left(-\frac{x}{\tau_i}\right)$. Future work will need to investigate eliminating negative Prony weights but also capping the maximum Prony time to enable the model to correctly predict the transition from aging to equilibrated behavior as seen experimentally. This particular challenge arises from the SPEC model implementation which uses just a single set of Prony times for both relaxation functions. In the research version of the SPEC model, implemented as the SPECTACULAR model, the relaxation functions may have independent Prony times, and this problem would not manifest.

In addition to yield strength, other measured and predicted changes associated with physical aging are discussed including the initial Young's modulus prior to yield and the strain at yield. The model data is generally smooth and well behaved as expected. Qualitatively, there is acceptable agreement between the model and experiments. However, the experimental data is quite noisy with respect to these two data measures, and so quantitative comparisons cannot be made at this time. Generally, the tangent Young's modulus and strain at compressive yield increased with aging time as expected.

Parametric studies were performed to asses the sensitivity of the aging time dependence of all three quantities of interest (yield stress, yield strain, and initial Young's modulus in compression). The parameter C3, which controls the volume strain (history) dependence of the shift factor and C4, which controls the change in the shift factor with shear deformation history, were varied by +/- 10% about the baseline values. The influence of these parametric studies on yield stress (Figure 11), yield strain (Figure 12), and initial tangent Young's Modulus (Figure 10) as well as the un-aged yield strength at different temperatures (Figure 16) were studied. With regard to aging behavior, C3 and C4 had a negligible effect on the initial tangent Young's modulus. Both C3 and C4 significantly changed the un-aged yield strength vs. temperature, but it appears that while changing these parameters can shift such curves,

they may not be able to re-shape the un-aged yield vs. temperature curve unless much larger changes in the parameters are explored. Similarly, with regards to aging behavior, C3 and C4 both impacted the un-aged datum for yield during 55 C aging. However, they did not significantly alter the slope of yield vs. aging time.

Underlying all of these changes is how the shift factor changes during aging. Figure 13 shows that the parameter C4 has no effect on the aging behavior as expected. Only C3 and the volumetric relaxation function (for a given thermal history to get into the glassy state) should impact this quantity. Over the parameter range sampled by C3, only small changes were observed in $\log_{10} a$ vs. aging time, and these changes manifested more strongly at early aging times. This finding suggests that C3 has a complicated role in the physical aging behavior in the absence of shear deformation.

What is missing from the parametric studies is the role of the volumetric relaxation function parameterization. Unfortunately, with the SPEC model UPM implementation, the Prony times are generally fixed to the shear relaxation function. Nevertheless, additional studies should be made on the breadth of that function (controlled by the KWW BETA1) parameter on the aging behavior predicted by the model.

In addition to a parametric study of C3 and C4, we also investigated the manually truncated volumetric relaxation function, f_1, that would force that relaxation function to equilibrate to its WLF limit at the same laboratory time scale observed experimentally in the yield strength evolution vs. aging time at 55 C. Details of this truncation are discussed at the start of section, 3.4. The truncated relaxation behavior does indeed equilibrate at the experimental time scale with respect to the shift factor evolution. But, truncating the volumetric relaxation function dramatically changes the glass forming behavior. The truncated material vitrifies at a significantly lower temperature during cooling than the baseline model, as manifested by acute discrepancies in the coefficient in thermal expansion behavior vs. temperature compared with experiments during cooling. This observation is evidence that for a given set of WLF parameters, longer relaxation time are required to more accurately simulate the vitrification process during cooling. The yield strength is much too large for all aging times and does not significantly evolve during aging. Clearly, a truncated relaxation function *is not* the mechanism by which the model can better predict the yield strength evolution.

At this point, we discuss on a potentially significant theoretical issue with the PEC and SPEC model. The model time-temperature shift behavior always equilibrates to the WLF limiting behavior given enough aging time, which for convenience we reproduce here,

$$\log_{10} \frac{\tau}{\tau_0} = \frac{-C_1 \left(T - T_0\right)}{C_2 + T - T_0}, \tag{1}$$

where C_1, C_2, and T_0 are material parameters with the last one typically set to a temperature near or above the glass transition temperature where the relaxation behavior of the material can surely be equilibrated. The parameter, τ_0, is the characteristic relaxation time scale at the reference temperature, T_0, and although Equation 1 is not how we typically write the

WLF equation for the SPEC model, this form is convenient in comparing to an alternative sub-Tg time-temperature shift model below. Clearly, when $T = T_0 - C_2$, the WLF equation diverges, and the equilibrated relaxation time is infinite. For the baseline 828DEA model, the shift factor diverges at 20.5 C (room temperature). Divergence, of course, means the model could never equilibrate, and below this temperature, the log of the shift factor is negative, which is nonsense (suddenly the model is equilibrating to a rubbery state!). Therefore, clearly, the WLF equilibration is a poor target deep in the glass for the shift factor.

But what should the shift factor equilibrate too? This question has been investigated relatively recently in the literature for more than fifty small molecule glass formers including both organic, such as 3-styrene, and inorganic glasses, such as soda lime silica glass [4]. That work found that an empirical function collapsed all of the different glasses onto a single curve of characteristic relaxation time relative to the relaxation time at a reference temperature, above the glass transition temperature with the following equation,

$$\log_{10} \frac{\tau}{\tau_0} = \left(\frac{J}{T_0}\right)^2 \left(\frac{T_0}{T} - 1\right)^2, \quad T_0 > T > T_x, \tag{2}$$

where J, T_0, and τ_0 are material parameters with the later two as the reference temperature near the glass transition and the characteristic relaxation time at that temperature. The authors in [4] discuss the anticipated domain of validity of Equation 2, which we reproduce and quote directly here: *"In particular, it [Equation 2] should not apply above a temperature of T_o, where excitations facilitating molecular motions are present throughout the system. In that regime, correlated dynamics is not required for molecular motions, and accordingly, temperature variation of transport is nearly negligible. The quadratic form should also not apply below another temperature, which we call T_x. The reasoning here recognizes that correlated dynamics leading to super-Arrhenius behavior is the result of constraints due to intermolecular forces. At an energetic cost, E, these constraints can be avoided. The time scale to pay that cost is $\tau_x \exp(E/T)$. While this time can be very long, at a low enough temperature, it will become shorter than a super-Arrhenius time. This is the temperature T_x, below which relaxation will be dominated by dynamics that avoid constraints."*

Thus, the quadratic time-temperature shift function discussed above applies only within a temperature range "near" the glass transition, and well below that temperature domain, the time-temperature shift is suggested to become Arrhenius. The determination of T_x is unclear from that work. Above T_0, any time-temperature shift model such as the Williams-Landel-Ferry Equation 1 is admissible though we conjecture that continuity of the equilibrated time-temperature shift behavior is required and may require some additional constraints on interfacing the quadratic form in Equation 2 with Equation 1.

The sub-Tg equilibrated time shift behavior was successfully used to described the very long time scale (20 million year) aging behavior of amber in [11], and the application of this model to polymeric materials has been noted as a worthwhile objective [7]. Such an alternative sub-Tg equilibrated time-shift model should be considered for enhancing the SPEC model to predict long-term physical aging behavior.

One more important consideration is what is our confidence in the baseline model calibration? The aging experiments shown in this report come from relatively recent work while the baseline model calibration is from data in [1]. Although the two materials are nominally the same, their behaviors are slightly different. Perhaps, if we had used a calibration from the more recent work, our results in this paper would have been different. A re-investigation of the baseline calibration is warranted.

In summary, the SPEC model does reasonably well in its baseline model in capturing the yield strength evolution of 828DEA for about 1000 hours, but the model continues to age for 6 additional decades beyond the experimentally equilibrate time scale. Parametric sensitivities were carried out, and the model was tweaked to understand such effects on the model response. However, aging behavior likely requires the model to equilibrate deep in the glass differently than the underlying WLF model contained in the SPEC model.

References

[1] D. B. Adolf, R. S. Chambers, and J. M. Caruthers. Extensive validation of a thermodynamically consistent, nonlinear viscoelastic model for glassy polymers. *Polymer*, 45(13):4599–4621, 2004.

[2] D. B. Adolf, R. S. Chambers, and M. A. Neidigk. A simplified potential energy clock model for glassy polymers. *Polymer*, 50(17):4257–4269, 2009.

[3] Gabriel Arechederra. Evolution of mechanical properties during structural relaxation of the 828/dea epoxy. Master's thesis, New Mexico Institute of Mining and Technology, 2017.

[4] Yael S. Elmatad, David Chandler, and Juan P. Garrahan. Corresponding states of structural glass formers. *The Journal of Physical Chemistry B*, 113(16):5563–5567, 2009.

[5] Hau-Nan Lee and M. D. Ediger. Interaction between physical aging, deformation, and segmental mobility in poly(methyl methacrylate) glasses. *The Journal of Chemical Physics*, 133(1):014901, 2010.

[6] John D. McCoy, Windy B. Ancipink, Caitlyn M. Clarkson, Jamie M. Kropka, Mathias C. Celina, Nicholas H. Giron, Lebelo Hailesilassie, and Narjes Fredj. Cure mechanisms of diglycidyl ether of bisphenol a (dgeba) epoxy with diethanolamine. *Polymer*, 105:243 – 254, 2016.

[7] Connie B. Roth, editor. *Polymer Glasses*. Number 978-1498711876. CRC Press, 1 edition, December 2016.

[8] William Scherzinger and Brian Lester. Library of advanced materials for engineering (lame) 4.44. UUR SAND2017-4015, Sandia National Laboratories, April 2017.

[9] Christian Sell and Gregory B. McKenna. Influence of physical ageing on the yield response of model dgeba/poly(propylene oxide) epoxy glasses. *Polymer*, 33(10):2103–2113, 1992.

[10] SIERRA Solid Mechanics Team. *Sierra/SolidMechanics 4.48 User's Guide*. Computational Solid Mechanics and Structural Dynamics Department Engineering Sciences Center Sandia National Laboratories, Box 5800 Albuquerque, NM 87185-0380, 4.48 (sand202018-2961) edition, March 2018.

[11] Jing Zhao, Sindee L. Simon, and Gregory B. McKenna. Using 20-million-year-old amber to test the super-arrhenius behaviour of glass-forming systems. *Nature Communications*, 4:1783 EP –, 04 2013.

Internal Distribution:

MS-0840	E. Fang	1554
MS-0840	B. Lester	1554
MS-0840	K. Long	1554
MS-0840	B. Reedlunn	1554
MS-0840	W. Scherzinger	1554
MS-0346	J. Bishop	1556
MS-0346	B. Elisberg	1556
MS-0346	S. Grutzik	1556
MS-0346	K. Ford	1556
MS-0889	E.D. Reedy	1556
MS-0888	J. McElhanon	1850
MS-0958	J. Kropka	1853
MS-0958	N. Wyatt	1853
MS-0889	C. Glen	1854
MS-0791	C. Tenney	6631
MS-9042	A. Brown	8432
MS-9042	J. Ostien	8343
MS-9042	B. Talamini	9261

External Distribution:

Professor J. McCoy
New Mexico Institute of Mining and Technology
Socorro, NM 87801
John.McCoy@nmt.edu

Dr. Robert S. Chambers
rschambabq@msn.com

Appendix 1: UPM Model '828DEA.txt'

```
###
### Universal Polymer model  ###  based on Matthew's new 828/DEA cured fit
###    828/DEA UPM properties New fit to T=-55, 23, 37, 59C compression data
###              T=-55C compression data ARE included in this fit
###
### 20180430 cmtenne
###     Tweaked Prony times 1-7 to eliminate negative coefficients.

begin property specification for material epoxy

    density         = 1176
    thermal log strain function = thermal_log_strain

    begin parameters for model universal_polymer
        bulk modulus   = 4.9E9     ## Pa
        shear modulus  = 0.94E9     ## Pa
        wwbeta 1 = 0.14
        wwtau 1  = 6               ## s
        wwbeta 2 = 0.0
        wwtau 2  = 0.0            ## s
        spectrum start time = 0
        spectrum end time = 0
        log time increment = 0
        bulk glassy 0 =  4.9E9     ## Pa
        bulk glassy 1 =  -1.2E7    ## Pa/K
        bulk glassy 2 =  0
        bulk rubbery 0 = 3.2E9     ## Pa
        bulk rubbery 1 = -1.2E7    ## Pa/K
        bulk rubbery 2 = 0
        volcte glassy 0 = 0.00017  ## 1/K
        volcte glassy 1 = 2e-07    ## 1/(K*K)
        volcte glassy 2 = 0
        volcte rubbery 0 = 0.0006  ## 1/K
        volcte rubbery 1 = 4e-07   ## 1/(K*K)
        volcte rubbery 2 = 0
        shear glassy 0 = 0.94E9     ## Pa
        shear glassy 1 = -2.3E6    ## Pa/K
        shear glassy 2 = 0
        shear rubbery 0 = 4500000  ## Pa
        shear rubbery 1 = 0
        shear rubbery 2 = 0
        reference temperature = 75.0  ## C
```

```
        wlf c1 = 16.5
        wlf c2 = 54.5
        clock c1 = 0
        clock c2 = 0
        clock c3 = 900
        clock c4 = 11600  ## 12000  ## 10180
        clock c5 = 0
        clock c6 = 0
        filler vol fraction = 0
        stress free temperature = 75.0   ## C
# Spectrum ID = 2
        relax time 1 = 1e-10              ## s
        relax time 2 = 1e-09
        relax time 3 = 1e-08
        relax time 4 = 1e-07
        relax time 5 = 1e-06
        relax time 6 = 3.16e-06
        relax time 7 = 1e-05
     # From the fit of Doug Adolf's Time Domain Data
        relax time 8 = 7.40568469e-05
        relax time 9 = 2.01533769e-04
        relax time 10 = 5.48441658e-04
        relax time 11 = 1.49249555e-03
        relax time 12 = 4.06158599e-03
        relax time 13 = 1.10529514e-02
        relax time 14 = 3.00788252e-02
        relax time 15 = 8.18546731e-02
        relax time 16 = 2.22754295e-01
        relax time 17 = 6.06189899e-01
        relax time 18 = 1.64964807e+00
        relax time 19 = 4.48925126e+00
        relax time 20 = 1.22167735e+01
        relax time 21 = 3.32459793e+01
        relax time 22 = 9.04735724e+01
        relax time 23 = 2.46209240e+02
        relax time 24 = 1.82334800e+03
        relax time 25 = 1.35031404e+04
        relax time 26 = 1.00000000e+05
     # End master curve fit. Pre-Post terms are for spectrum 1
        relax time 27 = 3.00000000e+05
        relax time 28 = 1.00000e+06
        relax time 29 = 1.00000e+07
        relax time 30 = 1.00000e+08
        f2 1 = 0.0
```

```
        f2 2 = 0.0
        f2 3 = 0.0
        f2 4 = 0.0
        f2 5 = 0.0
        f2 6 = 0.0
        f2 7 = 0.0
        f2 8 = 3.93700850e-02
        f2 9 = 3.50592766e-02
        f2 10 = 2.48889978e-02
        f2 11 = 2.35643287e-02
        f2 12 = 4.26437449e-02
        f2 13 = 8.75427041e-02
        f2 14 = 6.86175240e-02
        f2 15 = 1.23402885e-01
        f2 16 = 1.05035951e-01
        f2 17 = 1.28444338e-01
        f2 18 = 1.38126941e-01
        f2 19 = 9.62856703e-02
        f2 20 = 3.41063750e-02
        f2 21 = 3.38761809e-02
        f2 22 = 8.76326757e-03
        f2 23 = 7.78242408e-03
        f2 24 = 2.41470277e-03
        f2 25 = 7.42811067e-05
        f2 26 = 3.21772860e-07
        f2 27 = 0.0
        f2 28 = 0.0
        f2 29 = 0.0
        f2 30 = 0.0
    end parameters for model universal_polymer

end property specification for material epoxy
```

Appendix 2: Input Deck

```
begin sierra Compression of Aged Polymer

  title Compression of Aged Polymer

   begin feti equation solver feti
   end feti equation solver feti

### UNITS #####
```

```
#
###############
## Force       = Newtons
## Stress      = Pascals
## Mass        = Kg
## Length      = meters
## Temperature = Kelvin (C when relative temperatures are needed)
## Time        = seconds
## Density     = Kg/m^3
###############
#
#########################################################################
###                                                                   ###
### APREPRO  Inputs  and function definitions                         ###
###                                                                   ###
#########################################################################
## Conversion Factors
#

### These are the experimental dimensions and displacement rate
#{height_in = 1.12}  # inches
#{diameter_in = 0.56}  # inches
#{compression_rate_inpermin = 0.1}  # inches / minute


#{NominalStrainMax = 0.15}
#{T_anneal = 105.0}  # degrees C
#{t_anneal_hr = 0.5}  # hours
#{CoolRate_permin = 0.8}  # degrees C per minute
#{T_room  = 25}  # degrees C
#{t_room1_hr = 1.0}  # hours (between annealing and aging)
#{t_room2_hr = 1.0}  # hours (between aging and testing)
#{T_age = 55.0}  # degrees C
#{t_age_hr = 0.0}  # hours
#{t_age_equil_hr = 0.5}  # hours (between T_room and T_age)
#{t_test_equil_hr = 0.5}  # hours (from T_room to T_test)
#{T_test = 55.0}  # degrees C
#
#
## Convert to seconds
#{t_anneal = t_anneal_hr * 60.0 * 60.0}
#{t_room1 = t_room1_hr * 60.0 * 60.0}
#{t_room2 = t_room2_hr * 60.0 * 60.0}
#{t_age = t_age_hr * 60.0 * 60.0}
```

```
#{t_age_equil = t_age_equil_hr * 60.0 * 60.0}
#{t_test_equil = t_test_equil_hr * 60.0 * 60.0}
#
#
### These are the simulation dimensions and displacement rate
#{HOSIM = 1}       # m
#{AREA0 = 1.0*1.0} # m^2

## Derived parameters
#{NominalStrainPerSec = compression_rate_inpermin / height_in / 60.0}  # 1/seconds
#{DISPRATE_SIM = NominalStrainPerSec * H0SIM}    # meters / second
#{t_test = NominalStrainMax / NominalStrainPerSec}  # seconds
#{t_cool = (T_anneal - T_room) / (CoolRate_permin / 60.0)}  # seconds
#
#
## (Initial) Time Steps
#{dt_base     = 1.0E-4 }

###
### Temperature History
###

## Kludge if aging time shorter than equilibration time
# {if (t_age < t_age_equil)}
# {T_age = T_room}
# {endif}
## Subtract equilibration time from aging time
#{t_age = max(t_age - t_age_equil, 0)}

  begin definition for function applied_temperature_fun
    type is piecewise linear
    begin values
      {t0 = 0.0}                        {T_anneal}
      {t1 = t0 + t_anneal}              {T_anneal}
      {t2 = t1 + t_cool}                {T_room}
      {t3 = t2 + t_room1}               {T_room}
      {t4 = t3 + t_age_equil}           {T_age}
      {t5 = t4 + t_age}                 {T_age}
      {t6 = t5 + t_age_equil}           {T_room}
      {t7 = t6 + t_room2}               {T_room}
      {t8 = t7 + t_test_equil}          {T_test}
      {t9 = t8 + t_test}                {T_test}
    end values
  end definition for function applied_temperature_fun
```

```
###
### Displacement Rate History
###

  begin definition for function applied_disprate_fun
    type is piecewise constant
    begin values
      {t0}      0.0
      {t8}      {DISPRATE_SIM}
    end values
  end definition for function applied_disprate_fun


###
### Material Properties
###

  begin definition for function thermal_log_strain
    type is piecewise linear
    begin values
     -100.00   0.00
      500.00   0.00
    end values
  end definition for function thermal_log_strain

###
### Directions
###

  define direction x with vector 1.0 0.0 0.0
  define direction y with vector 0.0 1.0 0.0
  define direction z with vector 0.0 0.0 1.0

###
### Material Model Definitions
###

#{include("828DEA.txt")}

###
### Element Block Definitions
###
```

```
  begin solid section solid_1
    strain incrementation = strongly_objective
    formulation = selective_deviatoric
    deviatoric parameter = 1.0
  end solid section solid_1

  begin finite element model mesh1
    Database Name = block_SI.g
    Database Type = exodusII

    begin parameters for block block_1
      material epoxy
      model = universal_polymer
      section = solid_1
    end parameters for block block_1

  end finite element model mesh1

##########################################################################
###                                                                    ###
### ADAGIO Procedure                                                   ###
###                                                                    ###
##########################################################################

  begin adagio procedure Agio_Procedure

    ###
    ### Time Step Definition
    ###

    begin time control

      begin time stepping block pAnneal
        start time =  0.0
        begin parameters for adagio region adagio_region
          time increment = {dt_base}
        end parameters for adagio region adagio_region
      end time stepping block pAnneal

      begin time stepping block pAge
        start time =  {t3}
        begin parameters for adagio region adagio_region
          time increment = {dt_base}
        end parameters for adagio region adagio_region
```

```
      end time stepping block pAge

      begin time stepping block pRest
        start time =  {t5}
        begin parameters for adagio region adagio_region
          time increment = {dt_base}
        end parameters for adagio region adagio_region
      end time stepping block pRest

      begin time stepping block pPreLoad
        start time =  {t7}
        begin parameters for adagio region adagio_region
          time increment = {dt_base}
        end parameters for adagio region adagio_region
      end time stepping block pPreLoad

      begin time stepping block pLoad
        start time =  {t8}
        begin parameters for adagio region adagio_region
          NUMBER OF TIME STEPS = 1000
        end parameters for adagio region adagio_region
      end time stepping block pLoad

      termination time = {t9}

    end time control


##########################################################################
###                                                                    ###
### ADAGIO Region                                                      ###
###                                                                    ###
##########################################################################


    begin adagio region adagio_region
      use finite element model mesh1
      logfile precision = 7

#{include("output_commands.txt")}

      ###
      ### Boundary Conditions
      ###
```

```
# Platen Condition Only During Loading
      begin prescribed velocity
        node set = nset_y1
        direction = y
        function = applied_disprate_fun
        scale factor = -1.0
        active periods = pLoad
      end prescribed velocity

# 3 Symmetry Conditions
      begin fixed displacement
        node set = nset_y0
        components = y
        active periods = pAnneal pAge pRest pPreLoad pLoad
      end fixed displacement

      begin fixed displacement
        node set = nset_x0
        components = x
        active periods = pAnneal pAge pRest pPreLoad pLoad
      end fixed displacement

      begin fixed displacement
        node set = nset_z0
        components = z
        active periods = pAnneal pAge pRest pPreLoad pLoad
      end fixed displacement

# Applied Temperature History
      begin prescribed temperature
        function = applied_temperature_fun
        scale factor = 1.0
        include all blocks
      end prescribed temperature

###
### Solver definition
###

      begin adaptive time stepping
         cutback factor = 0.5
         growth factor = 1.1
```

```
         maximum failure cutbacks = 10
         target iterations = 30
         iteration window  = 10
         minimum multiplier = 1.0e-2
         maximum multiplier = {360000.0/dt_base}
         active periods = pAnneal pAge pRest pPreLoad
       end adaptive time stepping

       begin solver

         begin loadstep predictor
           type = scale_factor
           scale factor = 1., 0.0
         end loadstep predictor

         begin cg
           target relative residual = 1.0e-10
           target residual = 1.0e-6
           acceptable relative residual = 1.0E-7
           acceptable residual = 1.0E-5
           Maximum Iterations = 100
           Line Search secant
           iteration print  = 10

           begin full tangent preconditioner
               linear solver = feti
               #tangent diagonal scale = 1e-6
               iteration update = 10
               small number of iterations = 20
           end full tangent preconditioner
         end cg

       end solver

     end adagio region adagio_region

   end adagio procedure Agio_Procedure

end sierra Compression of Aged Polymer
```

1 Output Commands 'output.commands.txt'

```
       ###
       ### Output
```

```
      ###

#User Output
      # The reaction force will be postive in compression for nset_y0
      begin user output
        node set = nset_y0
        compute global FRAXIAL as sum of nodal reaction(y)
        compute at every step
      end user output

      begin user output
        compute global NOMSTRESS from expression "FRAXIAL/{AREA0}"
        compute at every step
      end user output

      begin user output
        node set = nset_111 # Single node
        compute global DELTAY as average of nodal displacement(y)
        compute global DELTAX as average of nodal displacement(x)
        compute at every step
      end user output

      begin user output
        compute global NOMSTRAIN from expression "DELTAY/{HOSIM}"
        compute at every step
      end user output

      begin user output
        node set = nset_111 # Single node
        compute global GTEMP as average of nodal temperature
        compute at every step
      end user output

      begin user output
        block = block_1
        compute global GlogU_I1 as average of element log_strain_invariant_1
        compute global Gloga as average of element loga
        compute at every step
      end user output


# Field Output
      begin Results Output output_adagio_region
        Database Name = %B.e
```

```
        Database Type = exodusII
        At Time 0, Increment = 6
        At Time {t8}, Increment = 1
        nodal Variables = displacement as D
        nodal Variables = reaction as R
        element Variables = stress as S
        element Variables = temperature as T
        element variables = loga as loga
        element Variables = UNROTATED_LOG_STRAIN as logU
        global variables = GTEMP as GTEMP
        global variables = NOMSTRAIN as NOMSTRAIN
        global variables = NOMSTRESS as NOMSTRESS
        global variables = GlogU_I1 as GlogU_I1
        global variables = Gloga as Gloga
        global variables = DELTAX as DELTAX
        global variables = DELTAY as DELTAY
      end results output output_adagio_region


# Heartbeat Output
      begin heartbeat ouput DATAHB
        stream name = %B.hb
        append = off
        precision = 10
        legend = on
        at step 0, increment = 1
        global time as TIME_(s)
        global timestep as tstep_(s)
        global NOMSTRAIN as NOMSTRAIN_(None)
        global NOMSTRESS as NOMSTRESS_(Pa)
        global GTEMP as TEMPERATURE_(C)
        global GlogU_I1 as logU_I1_(None)
        global Gloga as Gloga
        format=CSV #default
        labels=off
        timestamp format=""
      end heartbeat ouput DATAHB

# Heartbeat Output at the loading time
      begin heartbeat ouput DATAHB2
        stream name = %B.loading.hb
        append = off
        precision = 10
        legend = on
```

```
  at step 0, increment = 1
  start time = {t8}
  global time as TIME_(s)
  global timestep as tstep_(s)
  global NOMSTRAIN as NOMSTRAIN_(None)
  global NOMSTRESS as NOMSTRESS_(Pa)
  global GTEMP as TEMPERATURE_(C)
  global GlogU_I1 as logU_I1_(None)
  global Gloga as Gloga
  format=CSV #default
  labels=off
  timestamp format=""
end heartbeat ouput DATAHB2
```